

THE EFFECT OF HARMONICS ON A TWO-LIMB
INDUCTION TYPE OVERCURRENT RELAY

by

CHEE BONG CHAN

A dissertation submitted to the Faculty of Graduate Studies of
the University of Manitoba in partial fulfillment of the requirements
of the degree of

MASTER OF SCIENCE

© 1975

Permission has been granted to the LIBRARY OF THE UNIVERSITY OF MANITOBA to lend or sell copies of this dissertation, to the NATIONAL LIBRARY OF CANADA to microfilm this dissertation and to lend or sell copies of the film, and UNIVERSITY MICROFILMS to publish an abstract of this dissertation.

The author reserves other publication rights, and neither the dissertation nor extensive extracts from it may be printed or otherwise reproduced without the author's written permission.



ACKNOWLEDGEMENT

The author would like to express his thanks to Dr. G.W. Swift for his continuous guidance and encouragement in carrying out this analysis. The financial aid in the form of a research grant from Manitoba Hydro is gratefully acknowledged. And the patience of Miss Alice Ng in typing out this thesis is also deeply appreciated.

ABSTRACT

The object of this thesis was to extend the investigation of the effect of harmonics on induction disc overcurrent relay characteristics. A more elaborate approach was used. Starting with the development of an electric equivalent circuit for a CGE (IAC54B) relay, and differential equations, the actual torque and time of operation were predicted for different harmonic frequencies. The feasibility of the mathematical analysis was also tested with current waveforms composed of up to three harmonic components.

TABLE OF CONTENTS

	<u>PAGE</u>
LIST OF ILLUSTRATIONS	v
CHAPTER	
1 INTRODUCTION	1
2 SOURCES OF UNDESIRABLE HARMONICS	4
2.1 Frequencies other than the power frequency.....	4
2.2 Sources from HVDC Converter.....	4
2.2.1 Characteristic harmonics	4
2.2.2 Non-characteristic harmonics	7
2.2.3 Effectiveness of harmonic filtering	10
2.3 Sources from Conventional AC Systems	10
2.3.1 Transformers	10
2.3.2 Synchronous machines	11
2.3.3 Transient frequencies	11
2.4 General Remarks	13
3 ANALYSIS OF THE OVERCURRENT RELAY	14
3.1 Structure of the relay	14
3.2 Operating principle	14
3.3 Equivalent Circuit	18
3.4 Mathematical description of torque production	22
3.5 Differential torque equation	26
4 EXPERIMENTATION	30
4.1 Tests on the equivalent circuit	30

<u>CHAPTER</u>		<u>PAGE</u>
	4.2A Measurement of the electromagnetic torque	30
	4.2B Another method for the torque measurement /.....	36
	4.3 Measurement of time characteristics	39
	4.4 General Remarks	40
5	CONCLUSIONS	48
	BIBLIOGRAPHY	50
APPENDICES		
A	Calculation of Magnetic and Electric Equivalent Circuit Components	52
B	Numerical Values of Other Parameters	54

LIST OF ILLUSTRATIONS

<u>FIGURE</u>		<u>PAGE</u>
2.1	Connection of HVDC converter to ac system	5
2.2	AC current wave shape with star/star converter transformer	8
2.3	Variation of harmonics with unbalance factor	9
	a. star/star connection $\alpha = 10^\circ$, $X_c = 0.15$ p.u.	
	b. star/delta connection $\alpha = 10^\circ$, $X_c = 0.15$ p.u.	
	c. star/star connection $\alpha = 140^\circ$, $X_c = 0.15$ p.u.	
	d. star/delta connection $\alpha = 140^\circ$, $X_c = 0.15$ p.u.	
2.4	Typical harmonic content of power system generator	12
3.1	Typical IAC relay mechanism in cradle with standard hinged armature instantaneous unit	15
3.2	Electromagnetic torque developed in an induction disk	16
3.3	Magnetic circuit of the induction relay	19
3.4	Electric equivalent circuit	20
4.1	Circuit diagram for testing validity of the equivalent circuit	31
4.2.1	Magnitude of induced voltage on the shaded pole-limb	32
4.2.2	Magnitude of induced voltage on the unshaded pole-limb	33
4.2.3	Ratio of shaded voltage/unshaded voltage	34
4.2.4	Phase difference between the induced voltages.....	35
4.3	Electromagnetic torque curves	37

<u>FIGURE</u>		<u>PAGE</u>
4.4	Measurement of the electromagnetic torque by a beam-balance	38
4.5	Circuit diagram of the measurement of the relay operating time	42
4.5.1 - 4.5.5	Comparison of predicted and measured time characteristics of different input currents	43
APPENDIX	A : Dimensions of the magnet and shading coil	55

CHAPTER 1

INTRODUCTION

Though less impressive, protective relaying is one of the important parts of the power system. It serves as a sort of insurance for the great investment involved in a power system. The function of a protective relay is to perform the direct tripping of circuit breakers, in order to remove as quickly as possible a faulty section involved in an electrical failure, mainly a short circuit and sometimes other abnormal behaviour which might cause damage to components or otherwise affect the effective operation of the rest of the system. Protective relays, however spend most of their lifetime sitting idle. It is therefore essential to ensure they will operate and do so correctly when faulty conditions are encountered. In brief, the criteria of a reliable relay are its sensitivity (the ability to distinguish abnormality from normal operation), selectivity (selection between conditions whether tripping of circuit breakers is required) and speed (to operate within specified time).

So far, the electromagnetic type of protective relay has been proved satisfactory. Although there is a tendency of their being displaced by the transistor type of relays, for some electromagnetic relay such as the overcurrent induction disc type, the relative simplicity, its worldwide application and the rich experience acquired during the past years still render it a better choice for many years to come.

Nevertheless, the electromagnetic induction disc type of relay is inherently frequency sensitive. As early as in the 1930's, it was found distorted waveforms would delay operation. [10] In a conventional ac system, this frequency effect is not significant enough to bring in a reconsideration of the application of induction relays due to the negligible presence of harmonic contents. The recent incorporation of HVDC transmission links into the power system necessitates a further investigation into the frequency effects on these relays, because at locations neighboring the D.C. converter station, there is a subsequent increase in the harmonic contents. Tests had already been done to various type of induction relays. [7] It was found that different relays were affected in different ways by waveforms composed of the same amount of harmonic distortions. The degree of deviation from their basic operation characteristic at 60 hertz is closely associated with their frequency response characteristics. Further research indicated a possibility of analysing this type of relay by its magneto-electric equivalent circuit. A Westinghouse CO-8 type overcurrent relay with an E shape electromagnet as its drive was analysed through its magneto-electric equivalent circuit, [6] and successfully accounted for a reversal of torque at higher frequencies and an increase in operation time or reduction in operating torque.

The sole purpose of this thesis is to extend the investigation of the frequency effect to an overcurrent induction disc type of electromagnetic relay (GE IAC 54B). Employing its magneto-electric equivalent

circuit, and the parameters of its components, it is possible to link the input harmonic content to the relay operating characteristic using the torque equation. And by superposition the operating time can be predicted for various waveforms composed of different harmonic contents. Actually the saturation of the electro-magnet can also be accounted for when higher multiples of pick-up current are considered, if the saturation curve is known. However, for simplicity, only the linear operating region of the electro-magnet is used, which is good enough for our purposes

In this analysis it is necessary to know the parametric values of various components of the protective relays not generally supplied by the manufacturer like the spring torque, the magnetic permeability of the electro-magnet, the magnetic constant of the damping magnet, inductance and resistance of the shading coil, and the disc, the moment of inertia of the disc, number of turns for different tap settings, dimensions and configuration of the components etc. Quite a bit of measurements and calculation are involved.

For relays of similar construction, this method is probably valid in the study of their reliability in the modern power system.

CHAPTER II

SOURCES OF UNDESIRABLE HARMONICS

2.1 Frequencies other than the power frequency

Relays are primarily designed for operation at the power frequency, as are most power system components. Nonetheless in practical operation on occasions they do come across various harmonics, transient harmonics, subharmonics, and sometimes oscillations of random frequency. These might have quite undesirable effects; not only on the performance of the protective relay itself, but also are to blame for interference in communication systems, excess losses in power machinery, lowering of power factor, and straining of electrical insulation in the system's hardware. The source of these undesirable frequencies is often the non-ideal operation of the system components above the knee of their magnetic saturation curve.

2.2 Source from HVDC Converters:

2.2.1 Characteristic harmonics

The advent of HVDC schemes has recently raised considerable concern about the excessive harmonic current waveforms created in the system. The greatest amount of harmonics arises from the converter operation itself. The rectifier and inverter are switching devices and so are different from any other type of ac system load. Under ideal conditions, with the ac supply voltage perfectly balanced, and the controlled pulses to the converter valves symmetrically spaced, there is still a characteristic distortion on the ac waveform, which can be shown by straightforward analysis. [4]

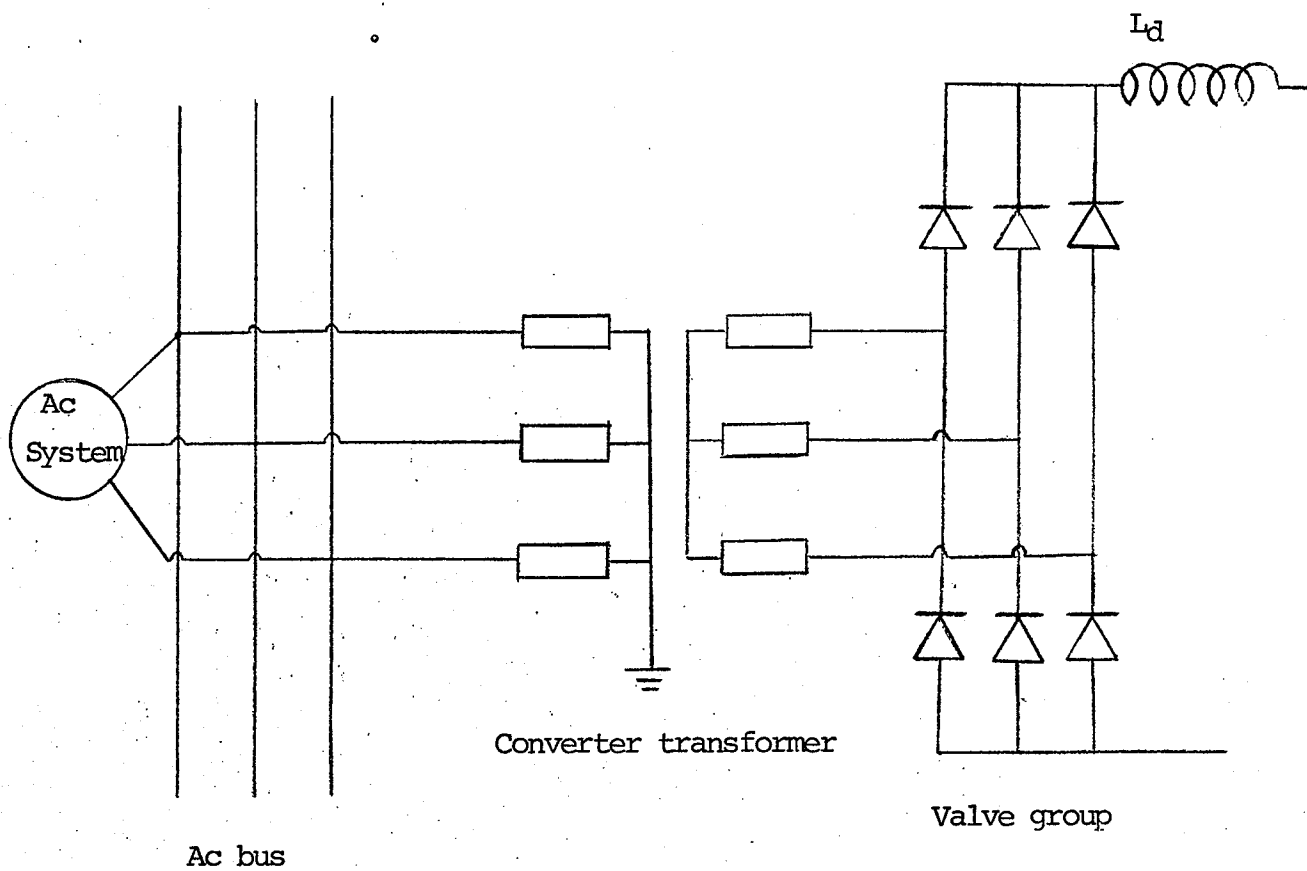


Figure 2.1: Connection of HVDC converter to ac system.

Assuming a zero commutation reactance and commutation angle neglected, the line current waveform for a delta/star (winding ratio = $\sqrt{3}:1$) transformer connection has a Fourier series as follows:

$$i = \frac{2\sqrt{3}}{\pi} \cdot I_d \left[\cos wt + \frac{1}{5} \cos 5 wt - \frac{1}{7} \cos 7 wt - \frac{1}{11} \cos 11 wt + \frac{1}{13} \cos 13 wt + \dots \right] \text{-----(2.1)}$$

A star/star (winding ratio = 1:1) transformer connection yields a current waveform of

$$i = \frac{2\sqrt{3}}{\pi} \cdot I_d \left[\cos wt - \frac{1}{5} \cos 5 wt + \frac{1}{7} \cos 7 wt - \frac{1}{11} \cos 11 wt + \frac{1}{13} \cos 13 wt + \dots \right] \text{-----(2.2)}$$

When two bridge units of equal capacity are working together in either series or parallel with one delta/star transformer of winding ratio ($2\sqrt{3}:1$) and the other a star/star transformer of winding ratio ($2:1$), the resultant current is given by

$$i = \frac{2\sqrt{3}}{\pi} \cdot I_d \left[\cos wt - \frac{1}{11} \cos 11 wt + \frac{1}{13} \cos 13 wt - \frac{1}{23} \cos 23 wt + \dots \right] \text{-----(2.3)}$$

where I_d is the dc line current.

The order of these characteristic harmonics can be expressed as

$$n = kp + 1$$

with a maximum magnitude of

$$I_n = I_1 / n$$

where k is a positive integer (1, 2, 3, 4,)

p is the number of pulses

With the presence of commutation reactance, which is actually the case, the magnitude of the harmonic currents is smaller than the maximum value. See figure (2.2)

It can be seen that harmonics entering the system can be greatly reduced by increasing the number of phases with which the converter operates, which is unfortunately not very practical beyond twelve pulses.

2.2.2 Non-Characteristic harmonics

When it comes to actual practise, harmonics other than those of the order $kp \pm 1$ are generated. This is the direct result of non-ideal operation. Under normal operation imperfect transposition and regulation of the ac system imposes a tolerance on the supposedly balanced nature of the commutating voltage, which is inevitable. In Figure (2.3) are typical examples of the magnitudes of uncharacteristic harmonics as a function of unbalance factor. The unbalance factor is defined as $\frac{-ve\ component}{+ve\ component}$. The unbalance of ac supply voltage mainly causes triplen harmonics. In this respect, the inverter operation is more sensitive than the rectifier operation. Another independent factor for the non-characteristic harmonics is the firing angle of the converters. Neither the inverse cosine nor the analogue automatic controls can completely eliminate a definite

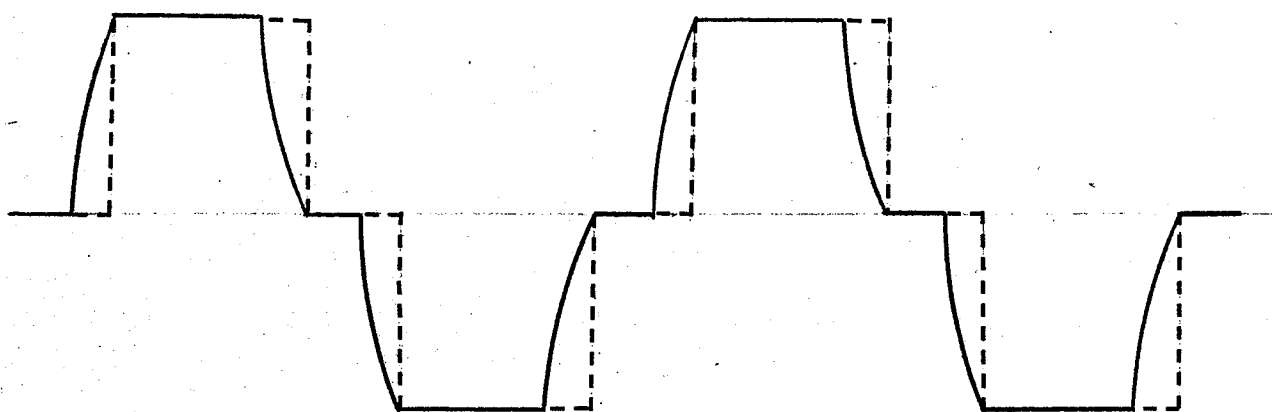


Figure 2.2: Ac current wave shape with star/star converter transformer.[4]

_____ Actual wave shape.

----- Wave shape with commutation reactance neglected.

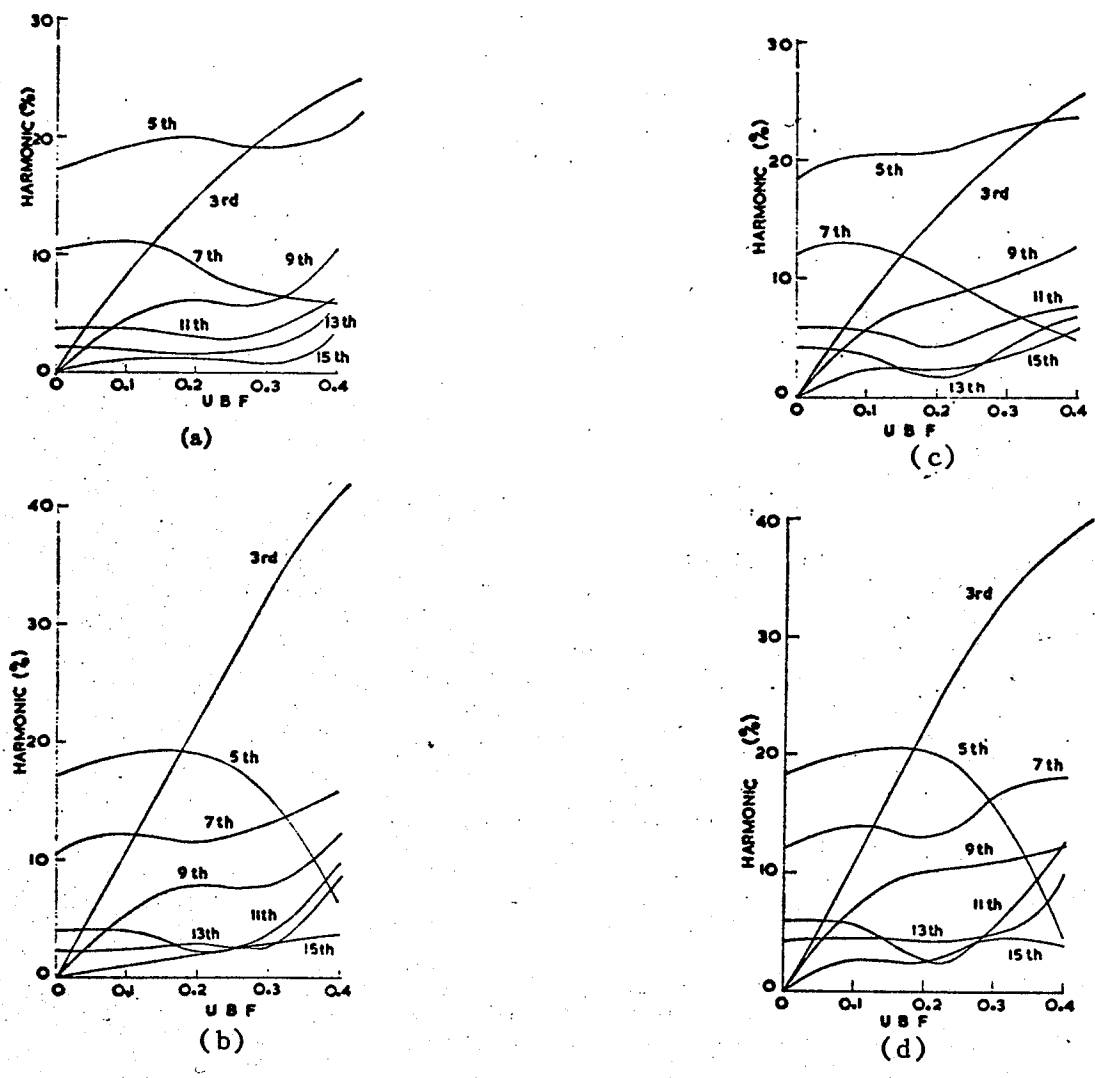


Figure 2.3; Variation of harmonics with unbalance factor [13]

- a, star/star connection, $\alpha = 10^\circ, X_c = 0.15 \text{ p.u.}$
- b, star/delta connection, $\alpha = 10^\circ, X_c = 0.15 \text{ p.u.}$
- c, star/star connection, $\alpha = 140^\circ, X_c = 0.15 \text{ p.u.}$
- d, star/delta connection, $\alpha = 140^\circ, X_c = 0.15 \text{ p.u.}$

degree of error which occurs at random. And just a tolerance of $\pm 0.25^\circ$ in firing angle, corresponding to 11 microseconds in a 60 hertz system can still give rise to significant noncharacteristic effects. As a consequence even harmonics with dc components are also generated.

2.2.3 Effectiveness of harmonic filtering

The effect of non-ideal converter operation can be of significant proportion in a large installation or in the case of heavy converter loading. It is not necessarily the magnitude of the harmonics generated which matters. For certain combinations of system components, harmonics propagated into the ac system can cause local or remote resonant over-voltage, which the existing ac filter designed for characteristic harmonics may not be capable of dealing with. In addition the characteristic dc component which cannot be filtered, in severe cases, could drive the transformer core into saturation.

2.3 Sources from conventional ac system

Besides the harmonics induced from converter operation, the conventional ac system itself is also contributing to harmonic content generally arising from nonlinearity of the system components.

2.3.1 Transformers

A transformer is usually designed to operate at the knee of its iron saturation curve for economic reasons. As a result, any increase in the normal operating voltage increases its degree of saturation and gives a distorted current waveform. Also the type of yoke construction and the mode of winding also have their role in this respect. For example,

a three phase core type transformer can reduce the third harmonic of the exciting current due to the high reluctance to the third harmonic flux; whereas a single phase transformer or a three phase shell type may have a third harmonic component as high as fifty percent of the fundamental voltage. A star/star winding connection with an ungrounded neutral suppresses triplen harmonic current flow whereas a grounded neutral suppresses the triplen harmonic voltage. And a parallel connection of a star connected bank with a delta connected bank will yield a reduction in the 5th and 7th harmonics. [18] A sending end transformer inductance and numerous line capacitances may be resonant to certain orders of harmonic frequency.

2.3.2 Synchronous machines:

Synchronous condensers, frequency converters, generators, and motors for industrial drives can be important potential sources of harmonics especially the synchronous generators which virtually supply all the electric power. Freedom from harmonics depends very much on the proper design and construction techniques. The number of slots, coil distribution, chord factor, skewing factor, and the magnetic materials used all have their bearing on the amount of harmonics induced. Today's commercial generators are relatively free from harmonic content. See Table (2.4) The only cause of practical concern is the possible series resonance at a particular order of harmonic between the machine reactance and a capacitive load.

2.3.3 Transient frequencies

Other frequency conditions such as those caused by lightning

HARMONIC	PHASE CURRENT (AMPS)			%OF
	A	B	C	FUNDAMENTAL
1	2880	3000	2880	100%
2	8.4	7.2	7.2	.24%
3	13.2	8.4	8.4	.28%
4	--	--	--	--
5	50.4	50.4	45.6	1.68%
6	--	--	--	--
7	13.2	13.2	13.2	.44%
11	1.92	1.32	1.68	.04%
13	8.4	8.4	8.4	.28%
17	8.8	9.0	8.9	.29%
19	1.8	1.8	1.9	.06%

Table 2.4 : Typical Harmonic Content of a Power [11]
System Generator

strokes and switching operations give rise to overvoltages of fundamental, harmonic and subharmonic frequencies. Magnetic inrush current contains a second harmonic of high magnitude. These are suitably controlled by artificial time delays, harmonic restraint filters, duplication of elements or subtleties in the art of application, so as to attain the required selectivity of a relay used.

2.4 : General Remarks

In the conventional ac system, the overall normal stray harmonics are relatively insignificant, with the 5th harmonic as the maximum, and yet having a magnitude of only a few per cent. Sixty five percent of the harmonics can be attributed to transformers, and the remainder to synchronous generators. Non-linear shunt reactor and induction motors have only negligible contribution. Under fault conditions, it is the air core leakage reactance which dominates, thus the waveform remains fundamentally sinusoidal. In a modern system, the aggravation of the harmonic content comes from HVDC schemes, which does not provide an exact conversion process from dc to ac and vice versa. The location affected most is the neighboring points to the converter station. Under some unfortunate circumstances the disturbing effect can occur at random.

CHAPTER III

ANALYSIS OF THE OVERCURRENT RELAY

3.1 Structure of the relay

The relay being analysed in this thesis is a CGE product, model number IAC 54B*. It is one of the relays employed to protect against overcurrent on single phase and polyphase circuits in utility and industrial electrical distribution systems, and frequently used in over-load back up protection. The heart of the device is an induction unit which is composed of : a laminated soft iron core wound by tapped copper coils, and shaded by copper coils on one limb of its terminating poles; a rotating aluminum disc mounted on a central shaft which cuts through the air gap between the poles of the C shape magnet; the central shaft also carries the moving contact which completes the trip circuit when it touches the stationary contact; a spiral spring is also attached to the shaft supplying a restraining and resetting torque; a permanent damping magnet gives further restraint to motion of the disk for appropriate time delay; jewel bearings are used on both ends of the shaft; also a small time dial setting disc for setting initial location of the aluminum disk to attain a correct timing.

3.2 Operating Principle

As all shaded pole structures⁺ are, it is operated by a single quantity input, ~~iee~~ the current flowing through the C.T. associated with the device. Since the magnitudes of faults depend mostly on their locations,

* see figure 3.1

+ see figure 3.2

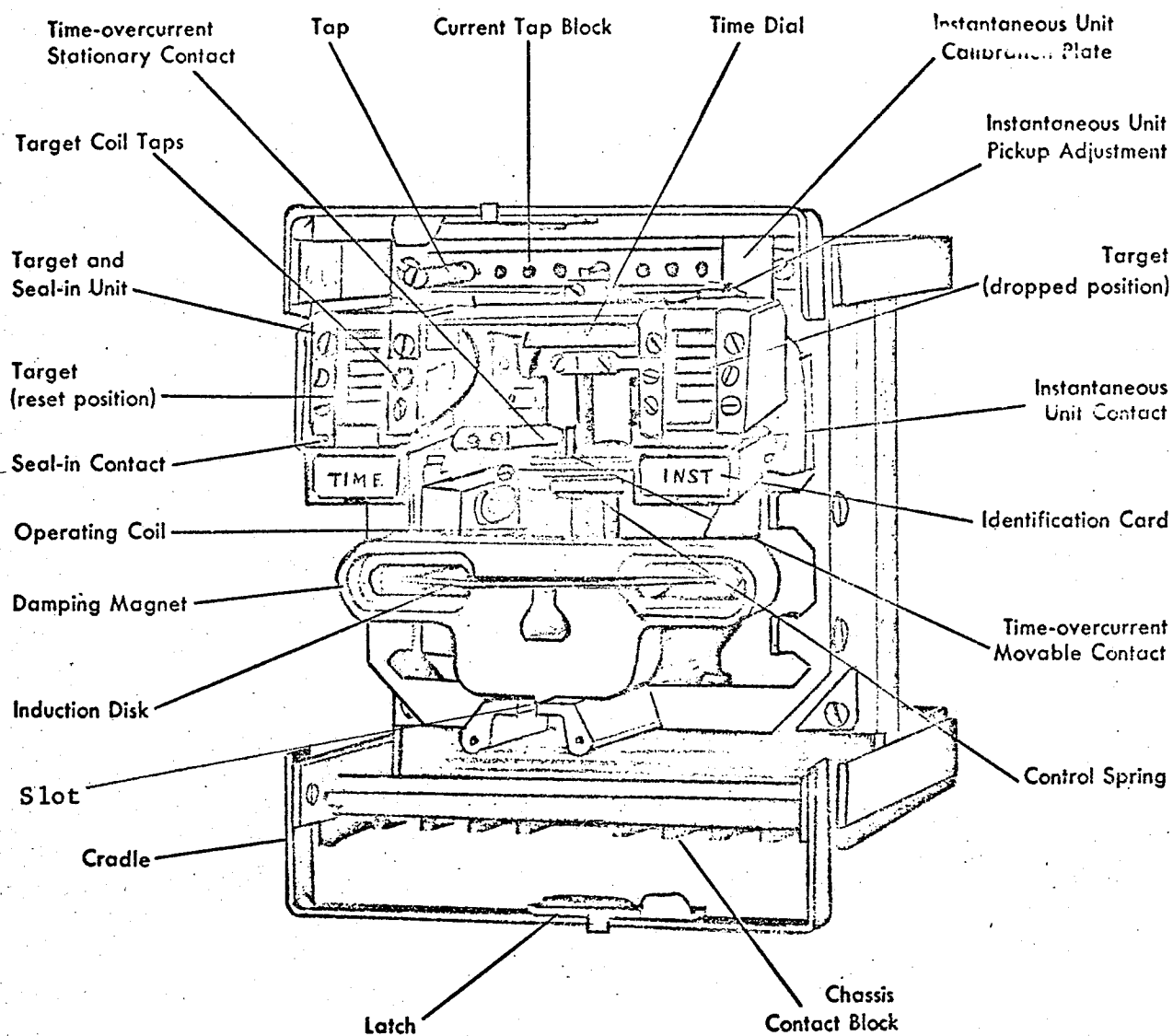


Figure 3.1 : Typical IAC relay mechanism in cradle with standard hinged armature instantaneous unit.

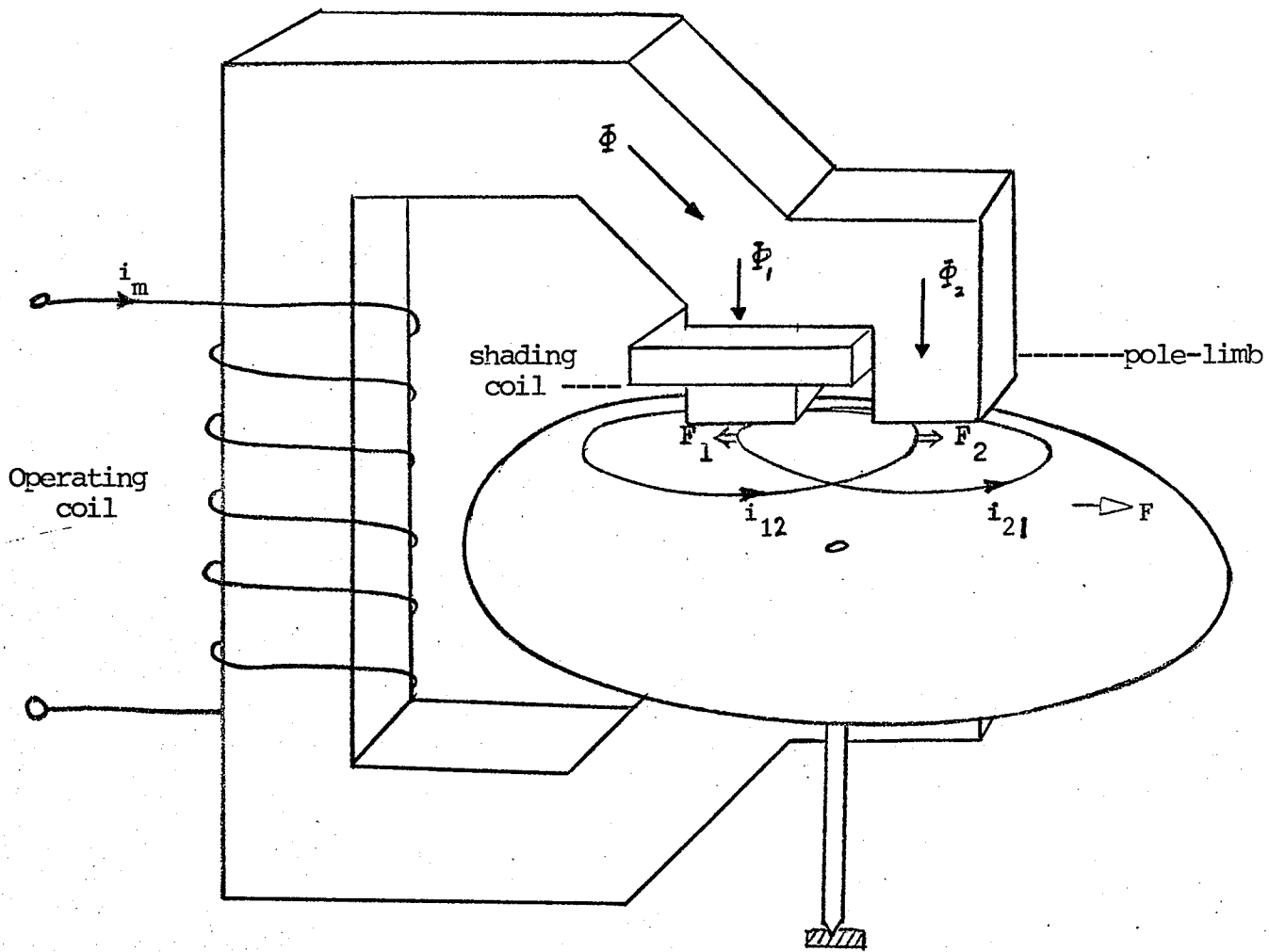


Figure 3.2: Electromagnetic torque developed in an induction disc.

the appropriate pick-up setting can be chosen accordingly by putting in the tap plug on the correct tap in the tap block. This in effect links a correct number of turns of copper coil wound on the electromagnet. Apart from a small amount of leakage, the electromagnetic fluxes induced are constrained to a path bounded by the laminated soft iron piece, and split into the terminating pole limbs. They then pass through the air gap and the aluminum disc directly under the poles. The laminated shading copper coil provides a required phase lag. Flux from each pole induces an eddy current flow in the disc, which in return reacts with flux from the other pole. Difference in the phase angle between the fluxes due to presence of the shading coil enables a net driving torque to develop. The spiral shape of the disc keeps the minimum tripping current constant by supplying more conducting portion of the disc under the poles to compensate for the increase in spring torque as the spring coil opens up. Actually the increase in spring torque is slight, and practically constant, whereas taking the spiral configuration of the disc into account might make the analysis unnecessarily complicated. The relay owes its accuracy mainly to the jewel bearings and precision parts that minimise friction. With a damping magnet as the major restraining torque producer, the relay disc always comes to a practically steady speed in a short time. Magnitude of the restraining torque can also be controlled by adjusting the location of the permanent magnet on its slot. This torque is proportional to angular speed, and the proportionality constant is a function of the strength of the magnet as well as its distance from the central shaft.

3.3 Equivalent Circuit

The analysis of the torque behaviour of the relay with respect to current magnitude and its frequency can be accomplished by utilizing its electric equivalent circuit (Figure 3.3). It is developed from the magnetic circuit by the duality theorem [5]. And the magnetic circuit (Figure 3.4) itself is based on actual calculation on the magnetic paths' lengths, effective cross-sectional areas and the magnetic permeabilities of the paths. Besides the components derived from the duality theorem, other components in the electric equivalent circuit are the actual electric components present in the relay. R_m is the resistance of the copper coil, R_i is the iron loss of the core. R_d is the resistance of the aluminum disc. R_{sc} is the resistance of the shading coil. L_{sc} is also an actual electric component calculated with respect to the shape and dimensions of the shading coil. Hysteresis and eddy current losses associated with the pole-limbs are neglected.

The nomenclature used in figures 3.3 and

3.4 is listed below :-

ϕ_m = the total flux produced

ϕ_L = the leakage flux

ϕ_1 = flux through the shaded limb

ϕ_2 = flux through the unshaded limb

R_m = the reluctance of the main portion of the electromagnet

R_s = the reluctance of the shaded pole-limb

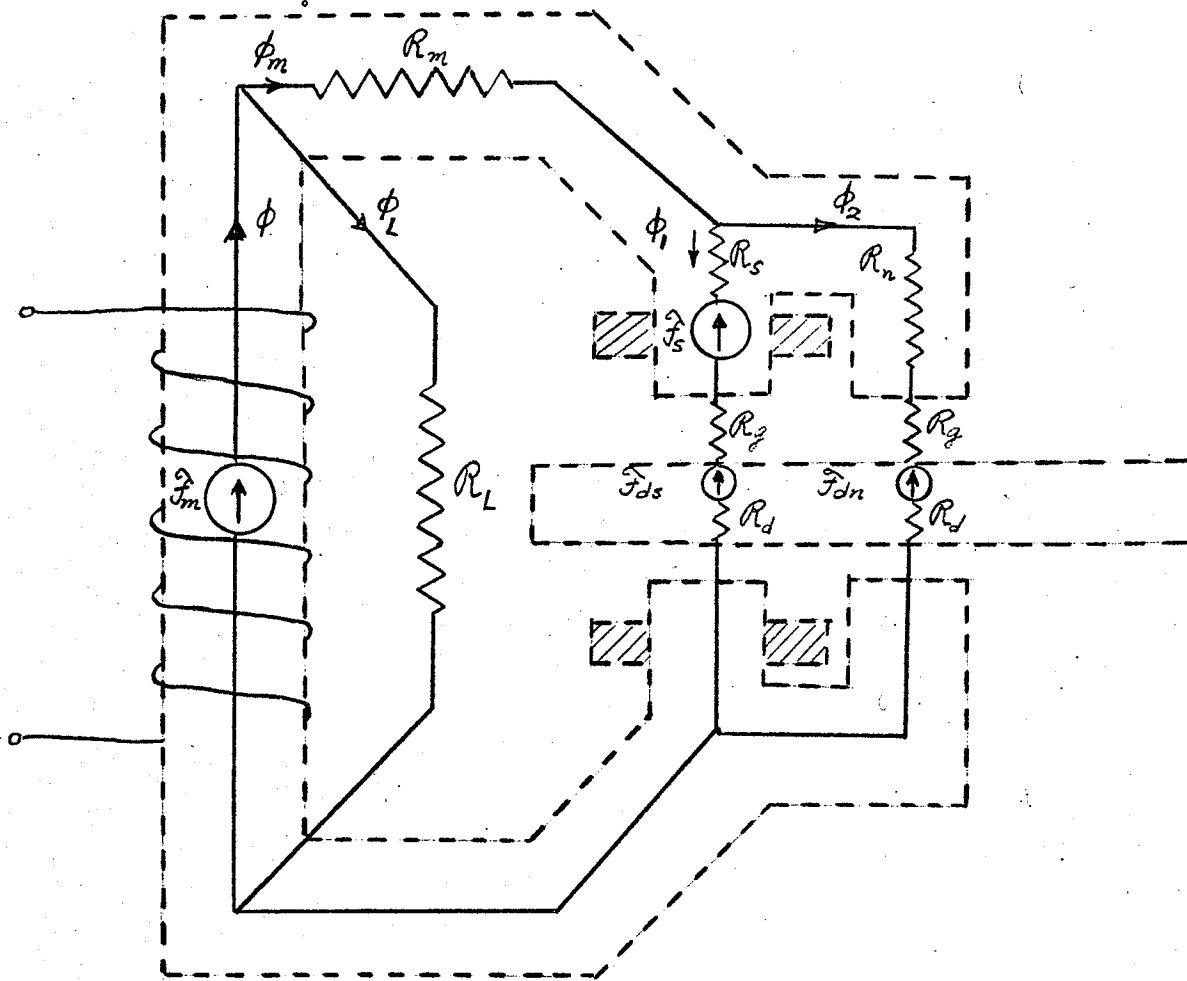


Figure 3.3: Magnetic circuit of the induction relay.

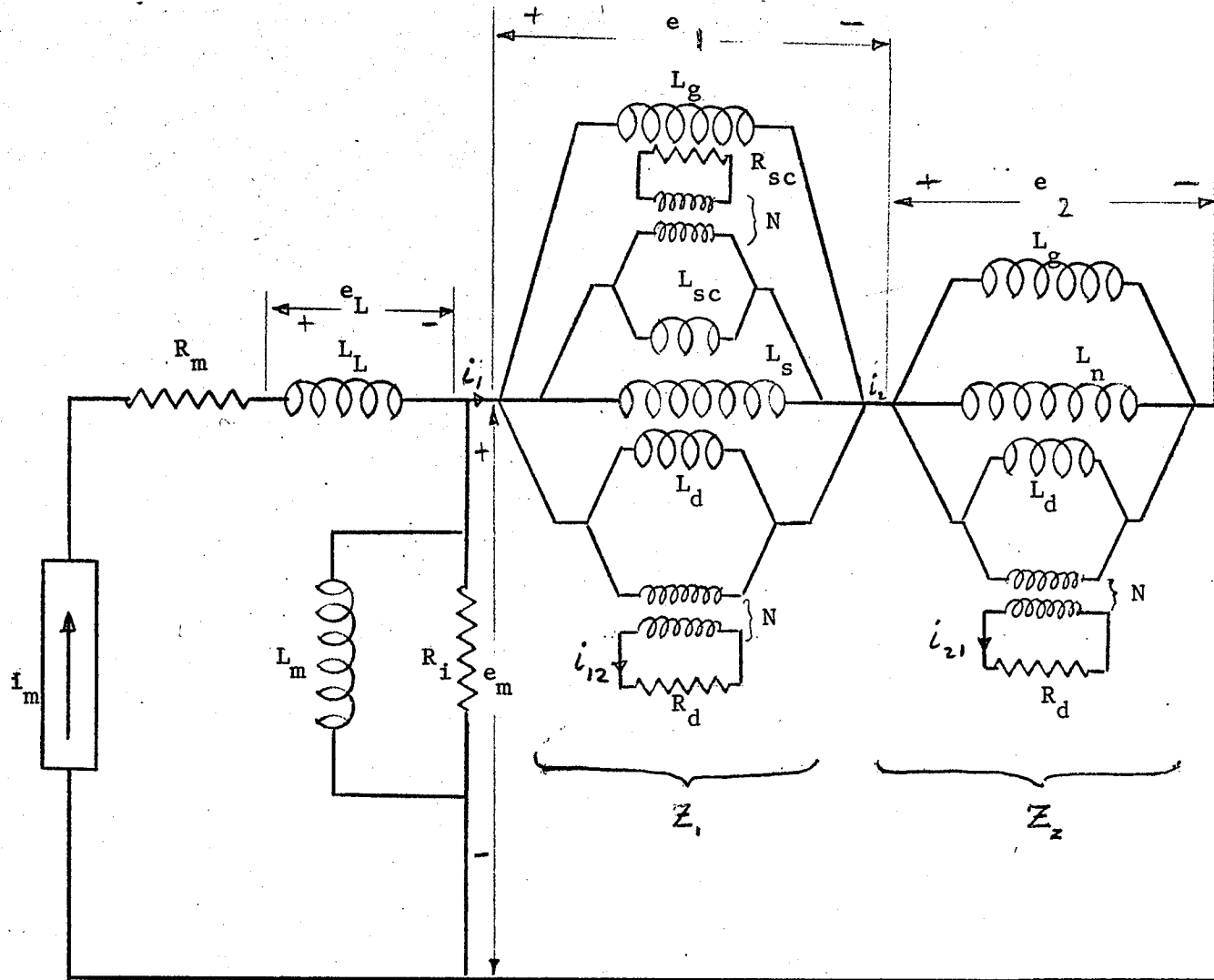


Figure 3.4 : Electric equivalent circuit

$\mathcal{R}_n =$ the reluctance of the unshaded pole-limb

$\mathcal{R}_g =$ the reluctance of the air gap

$\mathcal{R}_L =$ the leakage reluctance

$\mathcal{R}_d =$ the reluctance of the disc

$L_{sc} =$ inductance of the copper shading coil

$R_d =$ resistance of the disc

$R_s =$ resistance of the copper shading coil

The equations relating quantities in Figure 3.3 to those in Figure 3.4 are:-

$$\underline{e}_m = j \omega N \underline{\phi}_m \quad (\text{underlined variables are phasors})$$

$$\underline{e}_L = j \omega N \underline{\phi}_L$$

$$\underline{e}_1 = j \omega N \underline{\phi}_1 \dots\dots\dots(3.1)$$

$$\underline{e}_2 = j \omega N \underline{\phi}_2 \dots\dots\dots(3.2)$$

$$i_m = F_m / N$$

$$L_m = N^2 / \mathcal{R}_m$$

$$L_L = N^2 / \mathcal{R}_L$$

$$L_d = N^2 / \mathcal{R}_d$$

$$L_g = N^2 / \mathcal{R}_g$$

$$L_s = N^2 / \mathcal{R}_s$$

$$L_n = N^2 / \mathcal{R}_n$$

A digital computer program was written for the calculation of the electromagnetic torque produced by different harmonic current inputs. A further program was written superimposing up to three components of harmonics and comparing the predicted time of operation based on the torque produced and the differential equation discussed in the following sections.

3.4 Mathematical Description of Torque Production

From Warrington [2], the electromagnetic torque T_{em} is given by :

$$T_{em} = K_1 (i_{12} \phi_2 - i_{21} \phi_1) \dots \dots \dots (3.3)$$

where ϕ_1 = flux of the shaded pole

ϕ_2 = flux of the unshaded pole

i_{12} = disc current induced by the shaded pole and reacting with ϕ_2

i_{21} = disc current induced by the unshaded pole and reacting with ϕ_1

(ALL QUANTITIES INSTANTANEOUS)

$$\text{Assume } i_{12} = \hat{I}_{12} \cos (wt + \theta_{12}) \dots \dots \dots (3.4)$$

$$i_{21} = \hat{I}_{21} \cos (wt + \theta_{21}) \dots \dots \dots (3.5)$$

$$\phi_2 = \hat{\Phi}_2 \cos (wt + \theta_2) \dots \dots \dots (3.6)$$

$$\phi_1 = \hat{\phi}_1 \cos (wt + \theta_1) \dots \dots \dots (3.7)$$

where "hatted" quantities are phasor magnitudes, and θ 's are phasor angles.

Thus

$$\begin{aligned} T_{em} &= K_1 \left[\hat{I}_{12} \cos (wt + \theta_{12}) \hat{\phi}_2 \cos (wt + \theta_2) \right. \\ &\quad \left. - \hat{I}_{21} \cos (wt + \theta_{21}) \hat{\phi}_1 \cos (wt + \theta_1) \right] \\ &= K_1 \left\{ \hat{I}_{12} \hat{\phi}_2 \cdot \frac{1}{2} [\cos (2wt + \theta_{12} + \theta_2) + \cos (\theta_{12} - \theta_2)] \right. \\ &\quad \left. - \hat{I}_{21} \hat{\phi}_1 \cdot \frac{1}{2} [\cos (2wt + \theta_{21} + \theta_1) + \cos (\theta_{21} - \theta_1)] \right\} \\ &\dots \dots \dots (3.8) \end{aligned}$$

If we re-define T_{em} as the average torque, (which is the net torque driving the disc), then the double-frequency terms disappear, leaving

$$T_{em} = K_1 \left\{ \hat{I}_{12} \hat{\phi}_2 \cdot \frac{1}{2} \cos (\theta_{12} - \theta_2) - \hat{I}_{21} \hat{\phi}_1 \cdot \frac{1}{2} \cos (\theta_{21} - \theta_1) \right\} \dots \dots \dots (3.9)$$

Now let us make the simplifying assumption that

$$i_{12} = i_{21} \quad \text{and hence} \quad \hat{I}_{12} = \hat{I}_{21}, \quad \theta_{12} = \theta_{21}$$

The validity of this assumption will be borne out if test results are in reasonable agreement with calculations. Also, let $\theta_{12} (= \theta_{21}) = 0^\circ$, since one angle can always be set as an arbitrary reference.

Thus

$$T_{em} = \frac{K_1 \hat{I}_{12}}{2} [\hat{\phi}_2 \cos \theta_2 - \hat{\phi}_1 \cos \theta_1] \dots\dots\dots (3.10)$$

Referring to equations 3.1 and 3.2

$$\underline{e}_1 = j \omega N \underline{\phi}_1 \quad \text{and}$$

$$\underline{e}_2 = j \omega N \underline{\phi}_2$$

where these are PHASOR quantities

Thus, if \hat{E}_1 is the magnitude of e_1 and \hat{E}_2 is the magnitude of e_2 ,

$$\hat{E}_1 = \omega N \hat{\phi}_1 \quad \text{and}$$

$$\hat{E}_2 = \omega N \hat{\phi}_2$$

Therefore, equation 3.10 becomes

$$T_{em} = \frac{K_1 \hat{I}_{12}}{2} \left[\frac{\hat{E}_2}{\omega N} \cos \theta_2 - \frac{\hat{E}_1}{\omega N} \cos \theta_1 \right] \dots\dots\dots (3.11)$$

Referring to Figure 3.4

$$\underline{e}_1 = Z_1 \underline{i}_1 \quad \text{and}$$

$$\underline{e}_2 = Z_2 \underline{i}_2 \quad (\text{PHASORS})$$

Thus

$$\hat{E}_1 = Z_1 \hat{I}_1 \quad \text{and}$$

$$\hat{E}_2 = Z_2 \hat{I}_2$$

where

\hat{Z}_1 and \hat{Z}_2 are impedance magnitudes

We now make another assumption: that the disc currents i_{12} and i_{21} are pro-